Supporting Information

Synthesis and Structural Characterisation of Cu^{II}-based MOFs Constructed by Combining Functionalised 1,4-Bis(1*H*-Imidazol-1-Yl)Benzene Ligands with Copper Sulfate

Giulio Bresciani,[a,b,*] Massimo Guelfi,[a,b] Melodj Dosa,[c] Virginia Guiotto,[c] Valentina Crocellà,[c] Marco Lessi,[a,b] Marco Taddei[a,b,*]

[a] Università di Pisa, Dipartimento di Chimica e Chimica Industriale, Via G. Moruzzi 13, I-56124 Pisa, Italy.

[b] Centro per l'Integrazione della Strumentazione scientifica dell'Università di Pisa (C.I.S.U.P.), Università di Pisa, Pisa, Italy

[c] Dipartimento di Chimica, Centro Interdipartimentale NIS, Unità di Ricerca INSTM, Università di Torino, Via G. Quarello 15, I-10135 and Via P. Giuria 7, I-10125 Torino, Italy

Table S1. Crystal data and measurement details for **UdP-20, 21, 22** and **23**.

Compound	**UdP-20**	**UdP-21**	**UdP-22**	**UdP-23**
CCDC ID	2411960	2411961	2411962	2411963
Formula	$C_{19.5}H_{13.5}CuF_{4.5}N_6O_4S$	$C_{24}H_{18}Cl_2CuN_8O_4S$	$C_{26}H_{24}CuN_8O_4S$	$C_{26}H_{24}CuN_8O_6S$
FW, g/mol	576.96	648.96	608.13	640.13
T, K	150(2)	300(2)	300(2)	140(2)
λ, Å	0.71073	0.71073	0.71073	0.71073
Crystal system	Triclinic	Triclinic	Triclinic	Triclinic
Space group	*P*–1	*P*–1	*P*–1	*P*–1
a, Å	9.9888(5)	11.0780(5)	11.108(1)	12.3984(5)
b, Å	11.4316(5)	12.6235(6)	12.650(1)	12.6201(6)
c, Å	12.6577(7)	13.3342(5)	13.386(1)	14.2990(6)
α, °	104.810(2)	70.642(2)	70.221(4)	69.269(2)
β, °	94.908(2)	86.430(2)	86.430(4)	64.997(2)
γ, °	102.704(2)	85.269(2)	85.507(4)	64.189(2)
Cell Volume, Å^3	1347.6(1)	1752.1(1)	1763.4(3)	1785.3(1)
Z	2	2	2	2
D_c, g·cm^{-3}	1.422	1.230	1.145	1.191
μ, mm^{-1}	0.953	0.872	0.716	0.714
F(000)	580	658	626	658
Crystal size, mm	0.520x0.080x0.025	0.072x0.060x0.030	0.112x0.096x0.045	0.128x0.074x0.062
θ limits,°	1.90 to 26.07	1.93 to 25.02	1.92 to 25.74	2.02 to 25.07
Reflections collected	38992	56847	27253	61482
Independent reflections	5334 [R_{int} = 0.0619]	6174 [R_{int} = 0.1080]	6717 [R_{int} = 0.0665]	6309 [R_{int} = 0.0844]
Data / restraints / parameters	5334 / 6 / 334	6174 / 0 / 364	6717 / 0 / 366	6309 / 40 / 436
Goodness on fit on F^2	1.072	1.049	1.035	1.040
R_1 ($I > 2\sigma(I)$)	0.0763 (4150 data)	0.0545 (4521 data)	0.0430 (5054 data)	0.0671 (4956 data)
wR_2 ($I > 2\sigma(I)$)	0.2162 (4150 data)	0.1539 (4521 data)	0.1111 (5054 data)	0.1910 (4956 data)
R_1 (all data)	0.0913	0.0765	0.0605	0.0835
wR_2 (all data)	0.2297	0.1693	0.1195	0.2078
Largest diff. peak and hole, e Å^{-3}	2.104 / –1.655	1.097 / –0.999	0.454 / –0.335	1.249 / –0.650

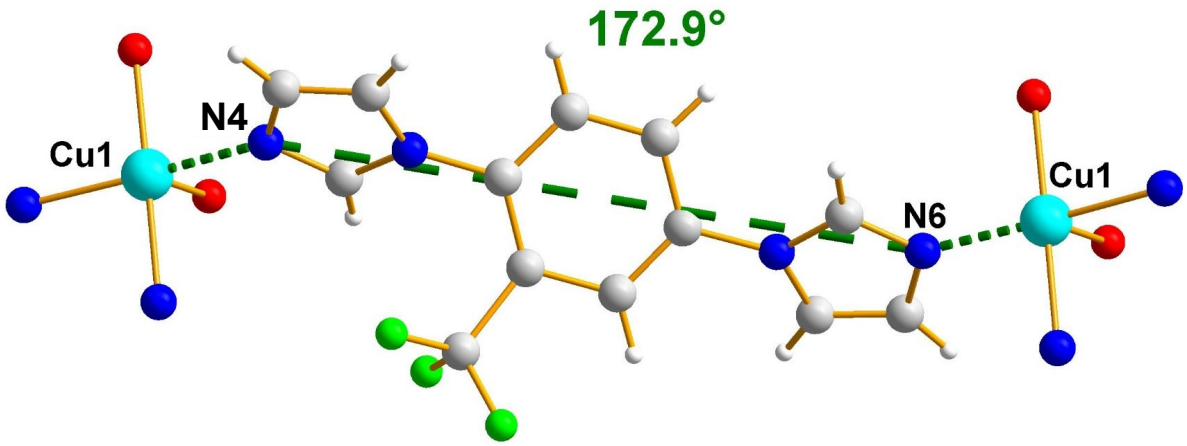

Figure S1. bibCF$_3$ ligand A in **UdP-20** adopts an *antiperiplanar* conformation with a 172.9° Cu-N-N-Cu torsion angle.

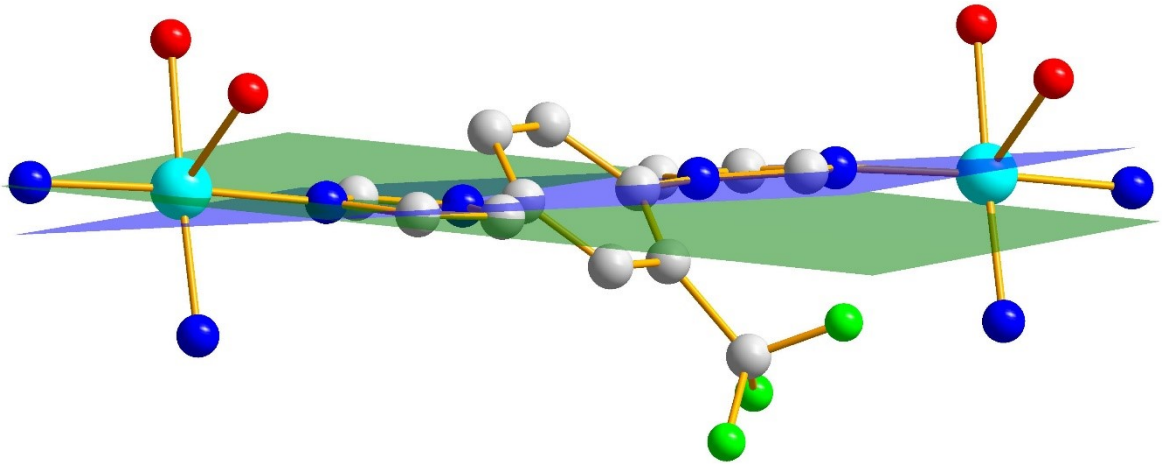

Figure S2. Dihedral angle (8.3°) between planes designed by the imidazole rings in **bibCF$_3$** ligand A in **UdP-20**.

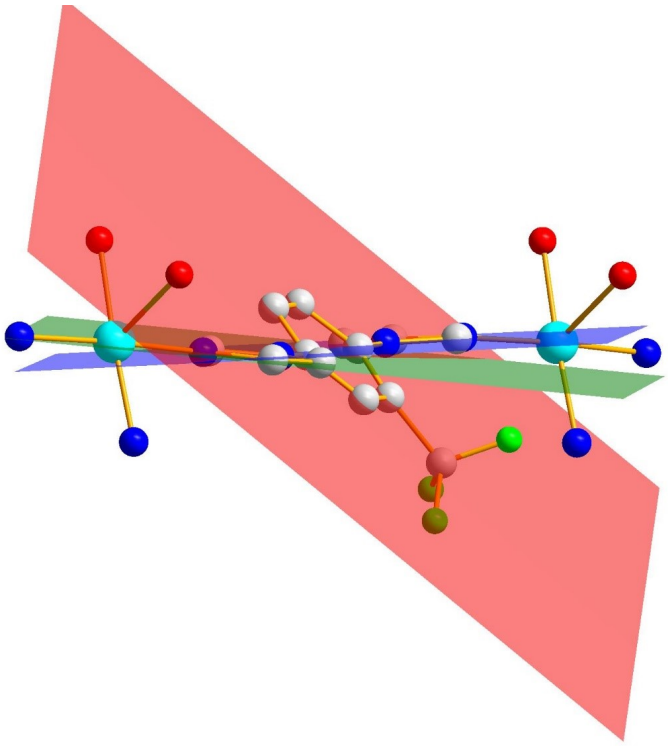

Figure S3. Dihedral angles of the benzene ring plane (red) with the imidazoles planes in **bibCF$_3$** ligand A in **UdP-20**: 46.5° (blue) and 38.5° (green).

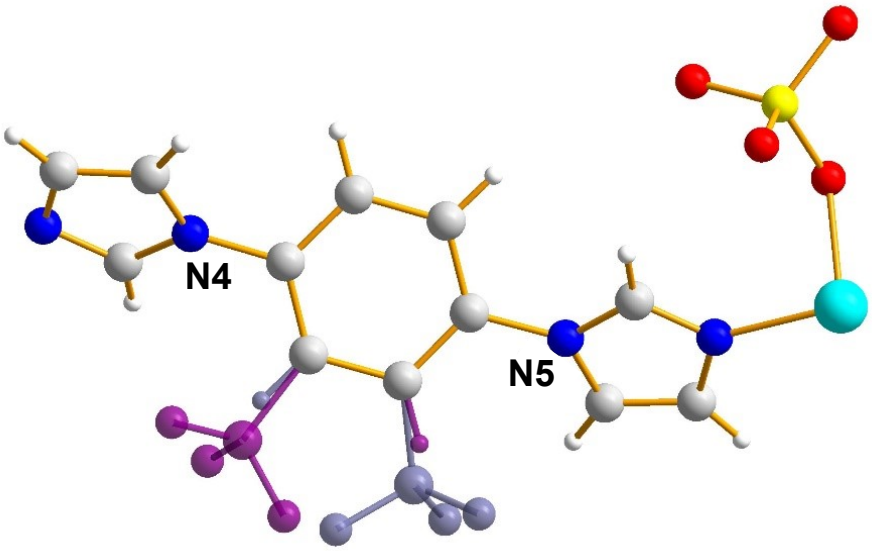

Figure S4. Positional disorder of CF_3 group on A ligand in **UdP-20**. Purple atoms possess 56% of occupancy.

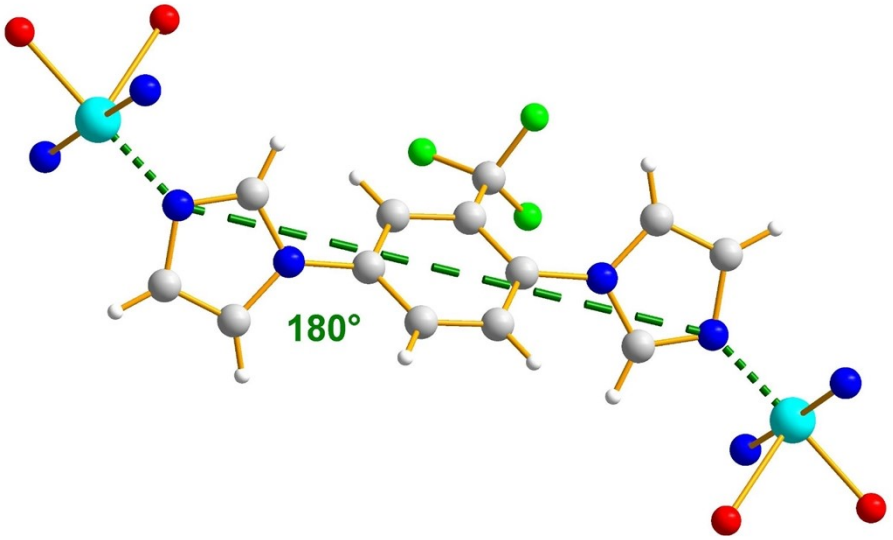

Figure S5. bibCF$_3$ ligand B in **UdP-20** adopts an *antiperiplanar* conformation with a 180° Cu-N-N-Cu torsion angle.

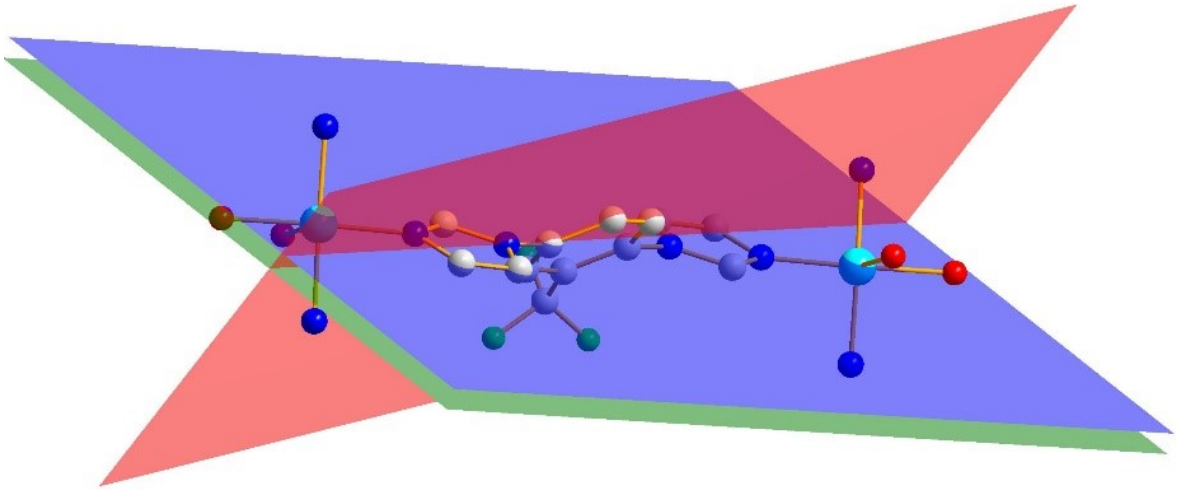

Figure S6. Dihedral angles of the benzene ring plane (red) with the imidazoles planes (blue and green) in **bibCF$_3$** ligand B in **UdP-20**: 49.9°.

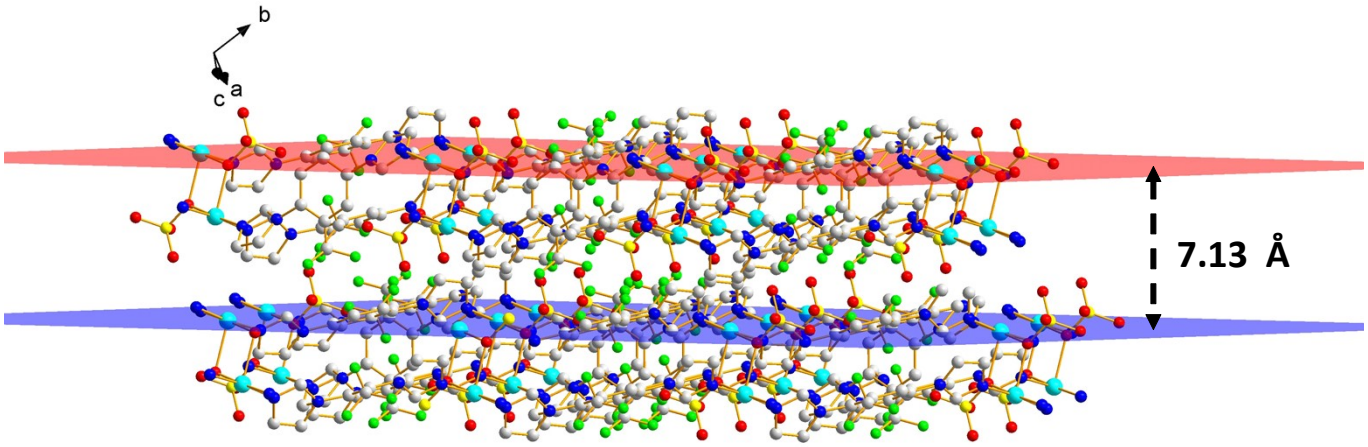

Figure S7. Interlayer distances in **UdP-20**.

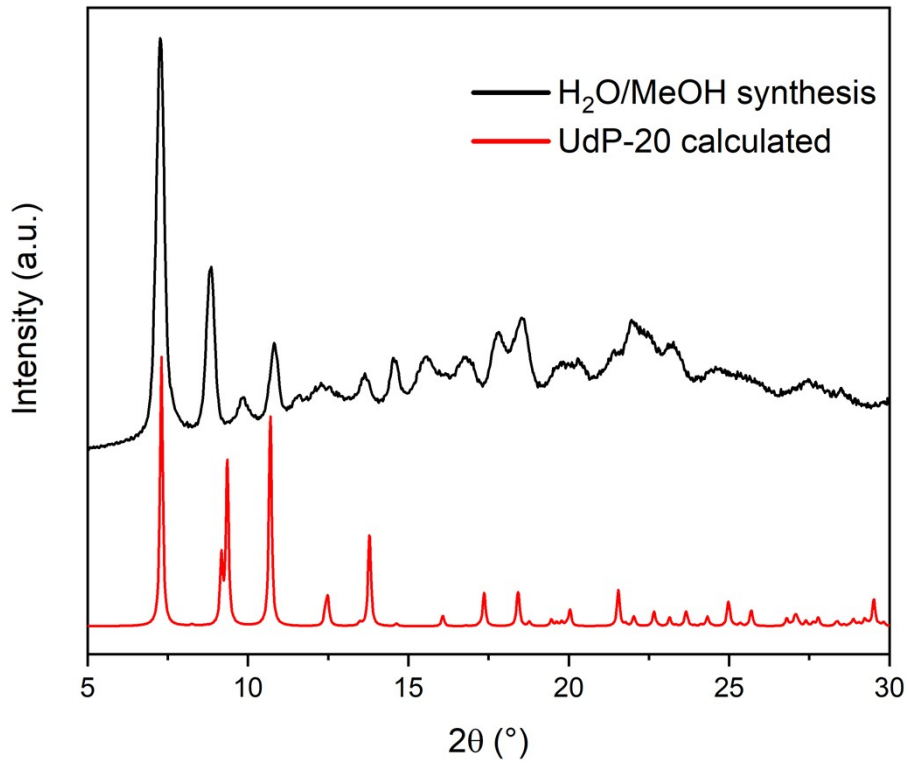

Figure S8. Comparison between calculated pattern of **UdP-20** (red) and powder pattern of product obtained from water/methanol synthetic approach (black).

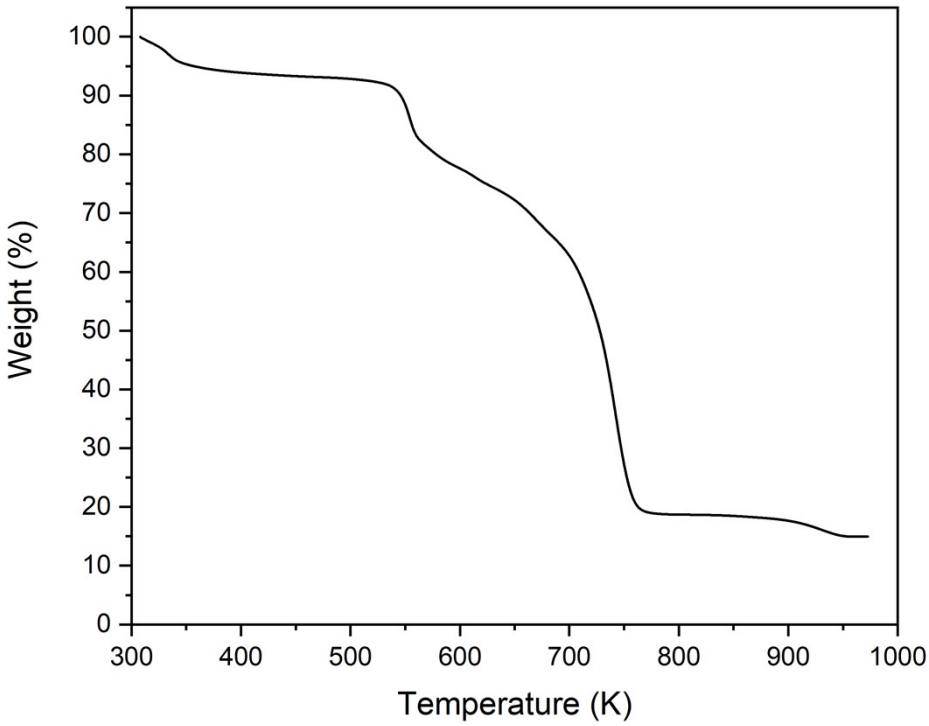

Figure S9. Thermogravimetric analysis of **UdP-20** under air.

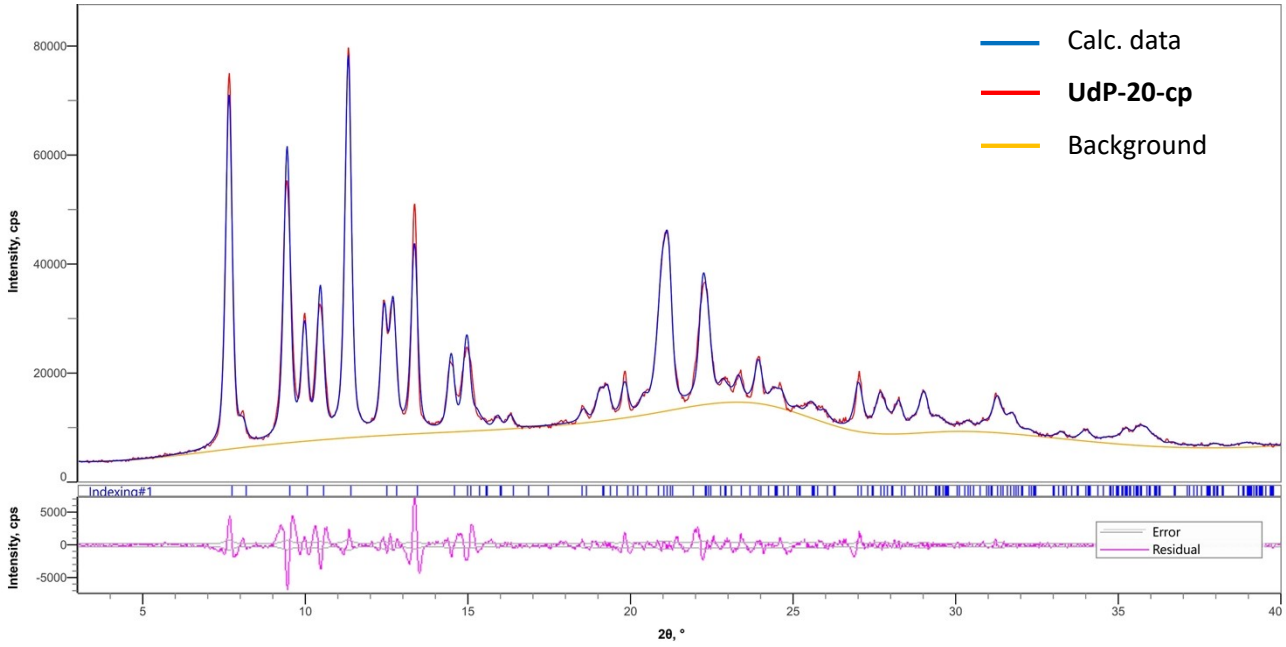

Figure S10. Whole powder pattern fitting of **UdP-20-cp**. Rwp: 4.84%

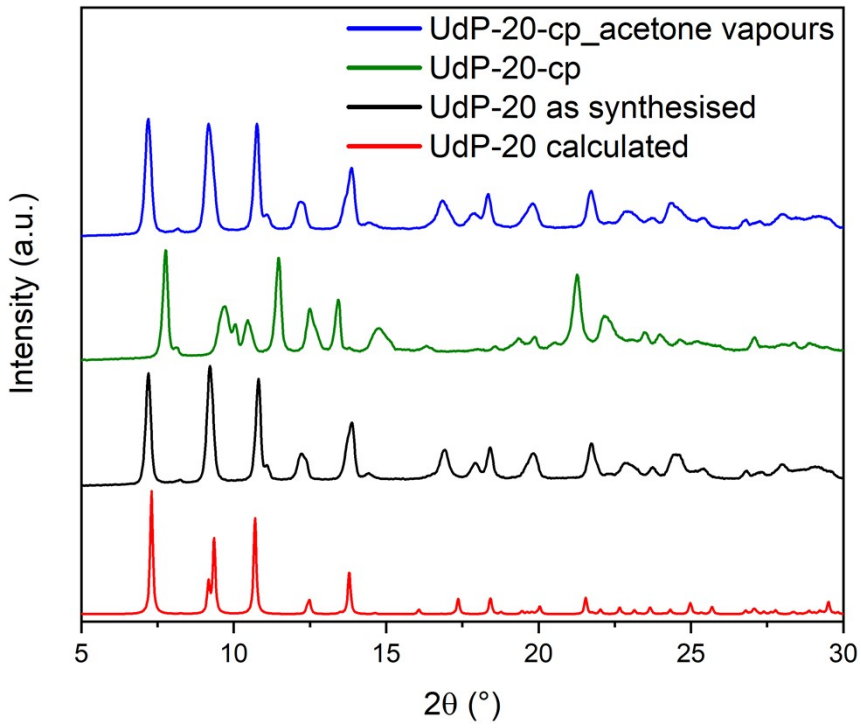

Figure S10. Comparison between PXRD patterns of **UdP-20** calculated (red), **UdP-20** as synthesised (black), **UdP-20-cp** (green) obtained by heating **UdP-20** at 353 K for 2 hours and **UdP-20-cp** exposed to acetone vapours overnight (blue).

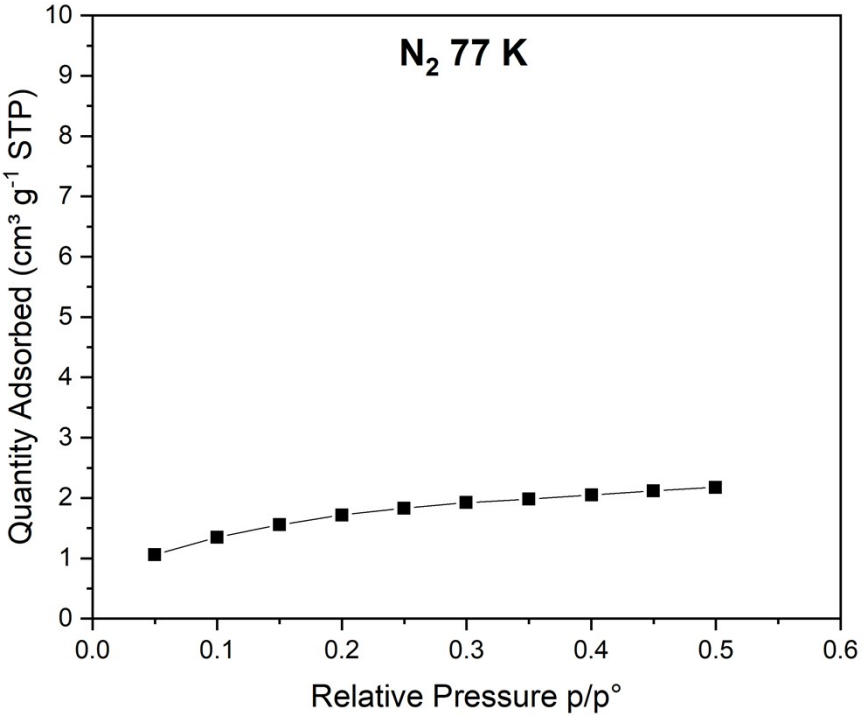

Figure S12. N_2 isotherm at 77 K of **UdP-20-cp**.

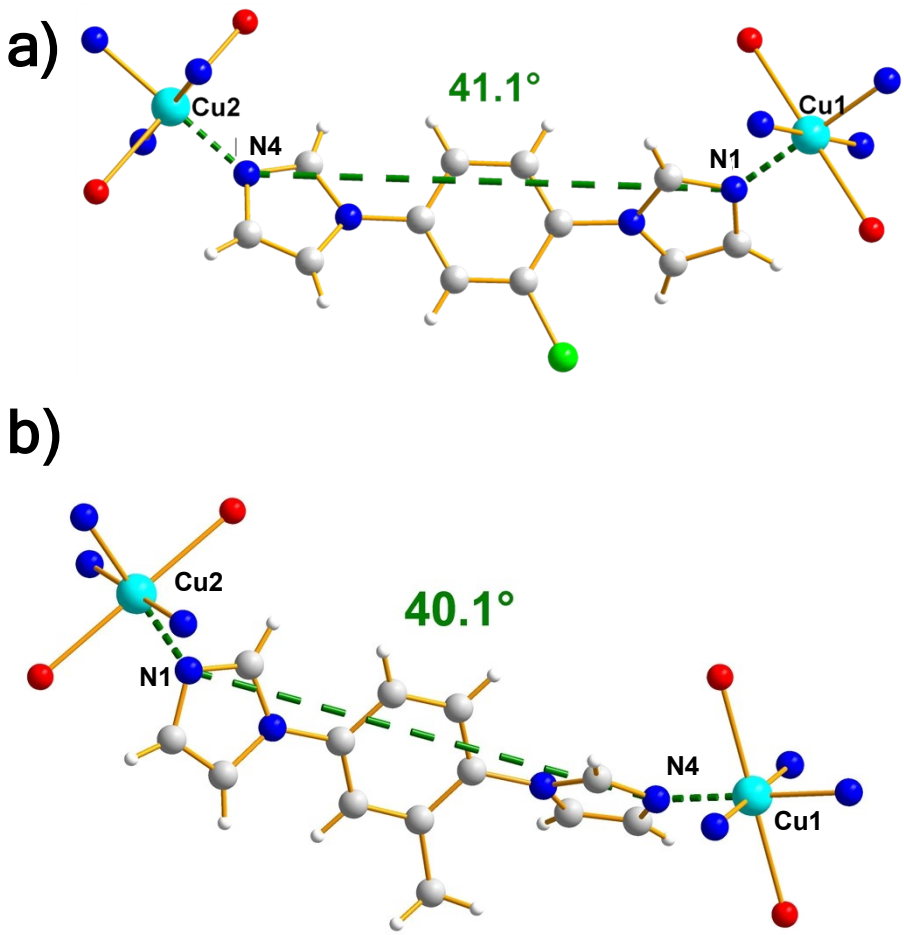

Figure S13. bibX ligand A adopting a synclinal conformation with Cu-N-N-Cu torsion angles of 41.1° in **UdP-21** (**bibCl**) **(a)** and 40.1° in **UdP-22** (**bibMe**) **(b)**.

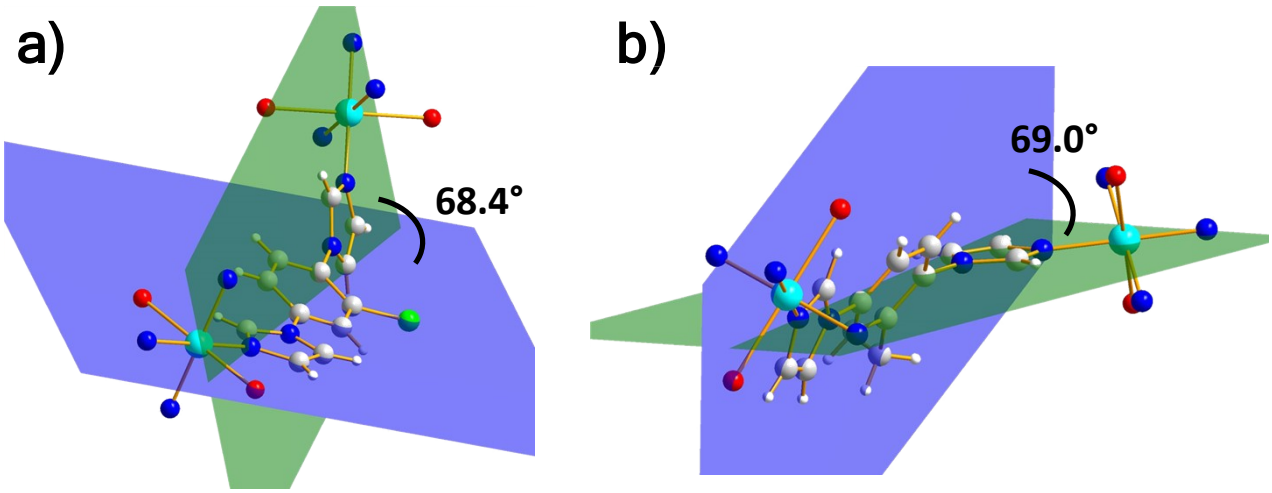

Figure S14. Imidazole planes in **bibX** ligand A (synclinal conformation) with dihedral angles of 68.4° in **UdP-21 (a)** and 69.0° in **UdP-22 (b)**.

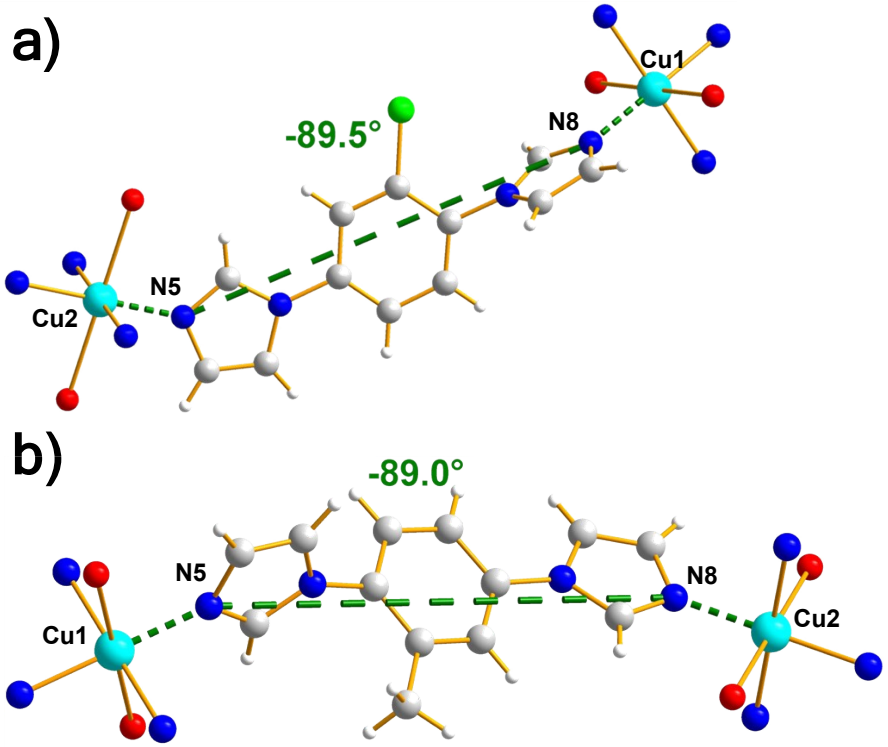

Figure S15. bibX ligand B adopting a synclinal conformation with Cu-N-N-Cu torsion angles of –89.5° in **UdP-21** (**bibCl**) **(a)** and –89.0° in **UdP-22** (**bibMe**) **(b)**.

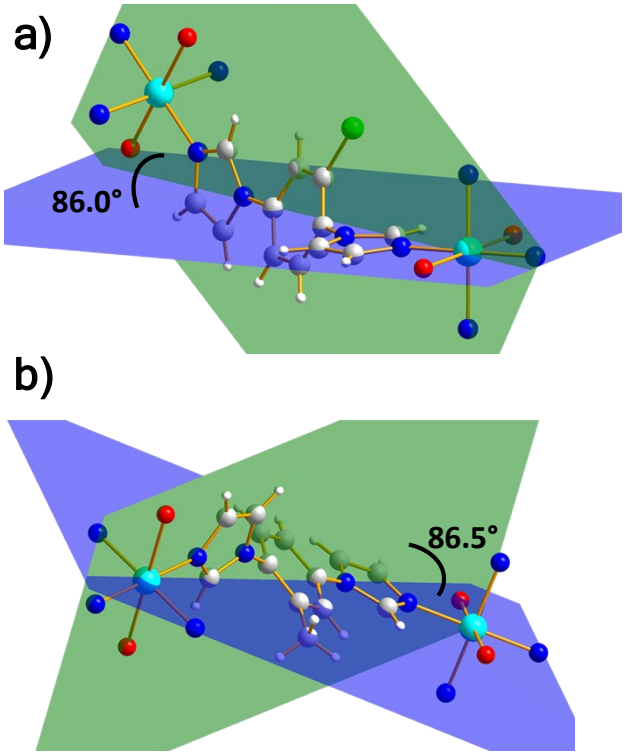

Figure S16. Imidazole planes in **bibX** ligand B (synclinal conformation) with dihedral angles of 86.0° in **UdP-21 (a)** and 86.5° in **UdP-22 (b)**.

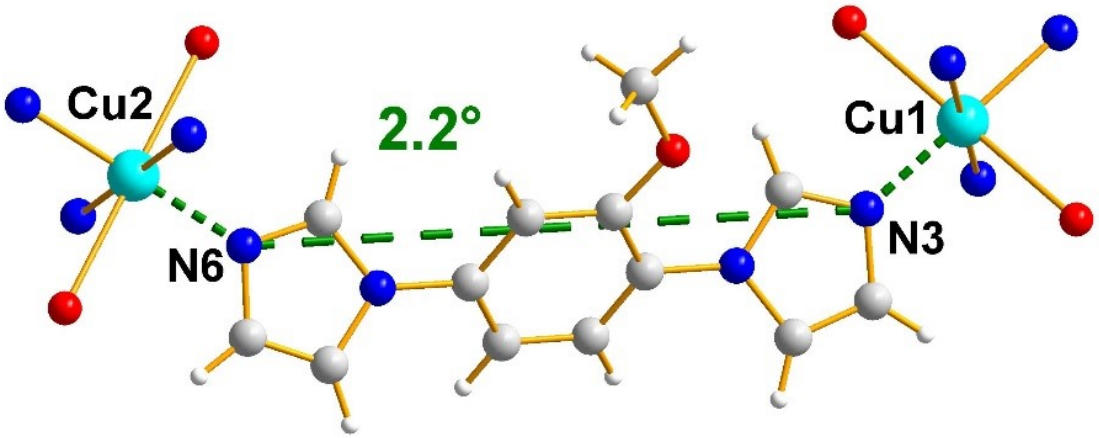

Figure S17. bibOMe ligand A in **UdP-23** adopting a syn conformation with Cu-N-N-Cu torsion angle of 2.2°.

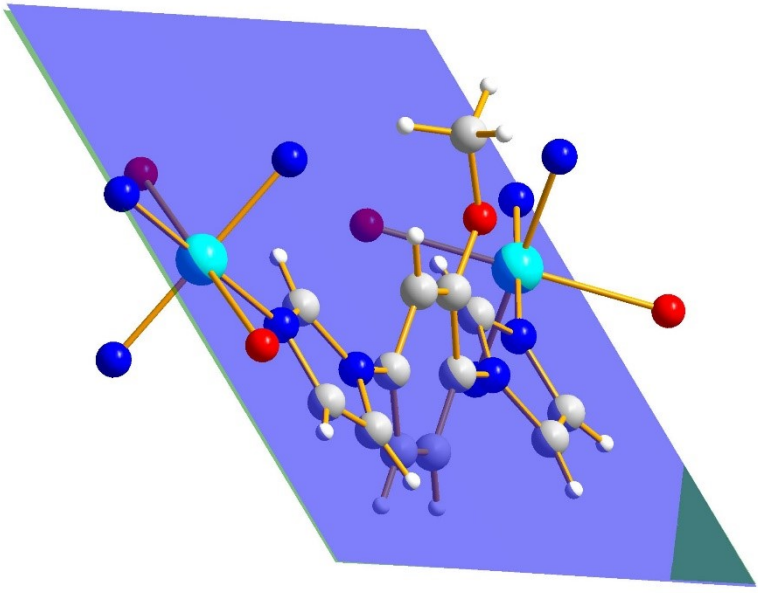

Figure S18. Imidazole planes in **bibOMe** ligand A (syn conformation) in **UdP-23** with dihedral angle of 0.3°.

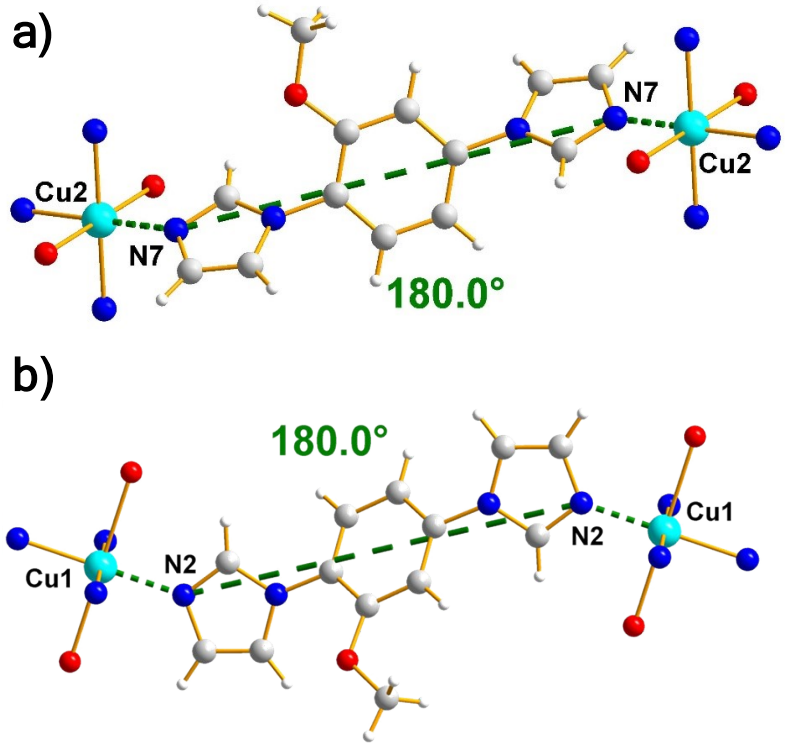

Figure S19. bibOMe ligand B **(a)** and C **(b)** in **UdP-23** adopting an anti conformation with Cu-N-N-Cu torsion angles of 180.0°.

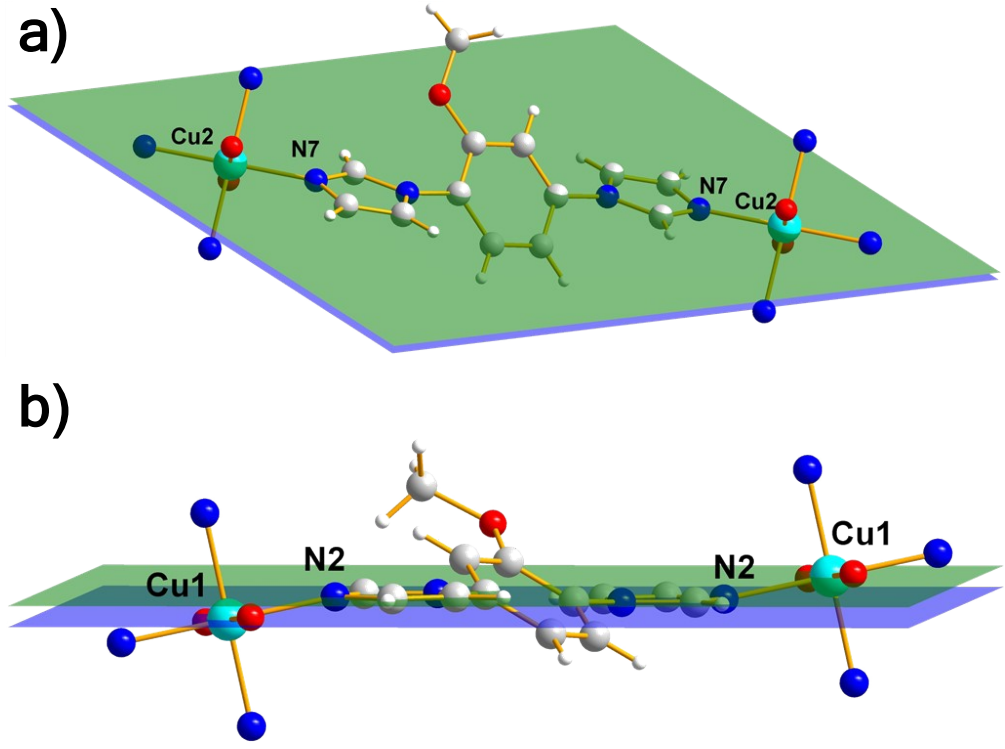

Figure S20. Parallel planes designed by imidazole rings in **bibOMe** ligand B **(a)** and C **(b)** (anti conformation) in **UdP-23** (dihedral angle of 0.0°).

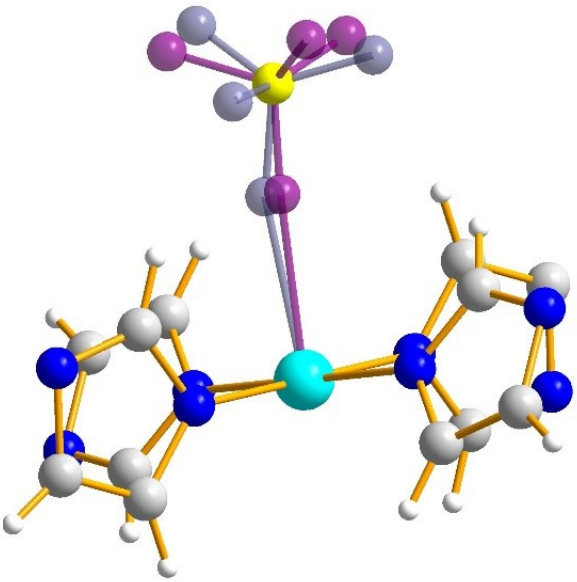

Figure S21. Disorder on two positions of SO_4 anion in **UdP-23**. Purple atoms posses 61% of occupancy.

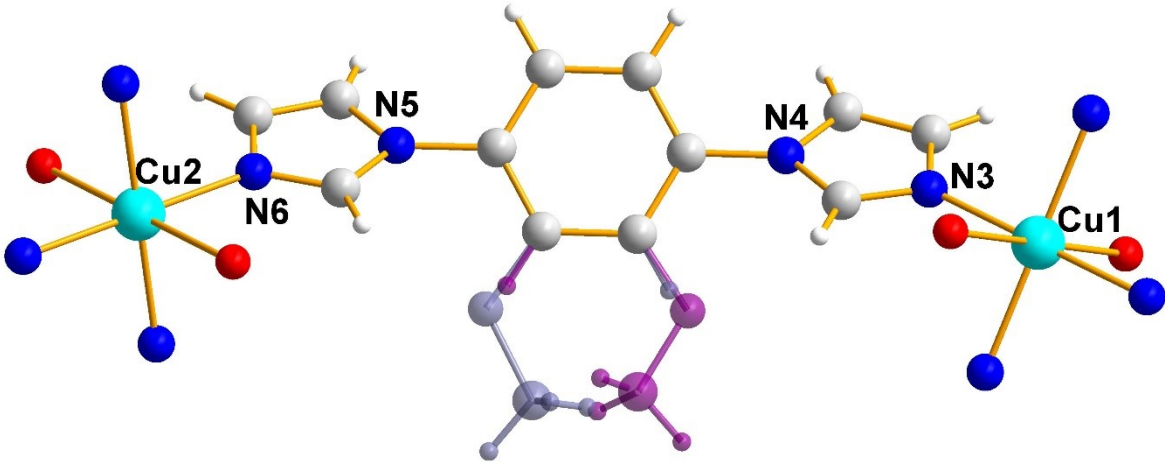

Figure S22. Positional disorder of OMe group on A ligand in **UdP-23**. Purple atoms posses 58% of occupancy.

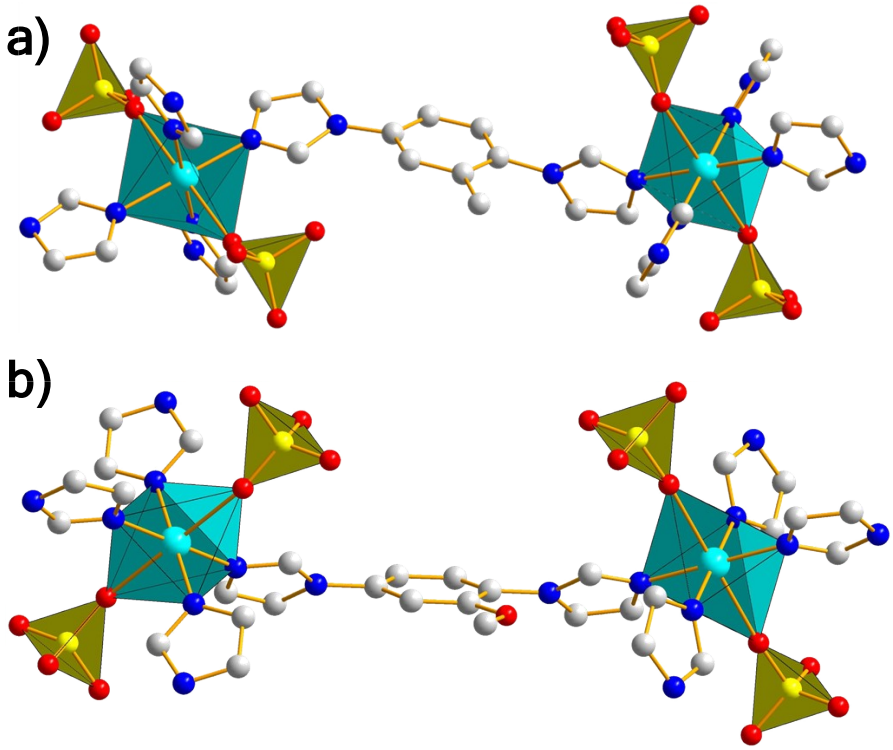

Figure S23. Copper and sulphur coordination environments in **UdP-22 (a)** and **UdP-23 (b)**.

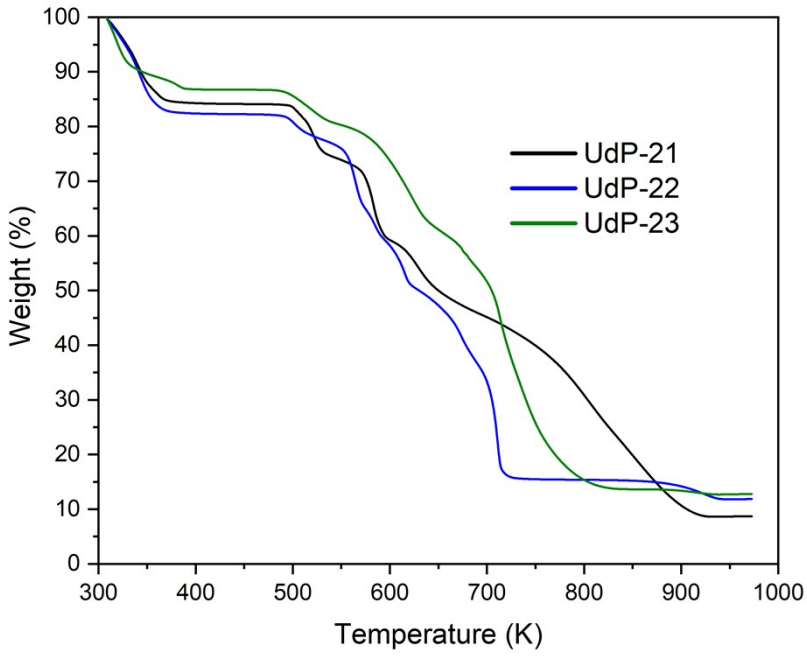

Figure S24. Thermogravimetric analysis in air of **UdP-21** (black), **UdP-22** (blue) and **UdP-23** (dark red).

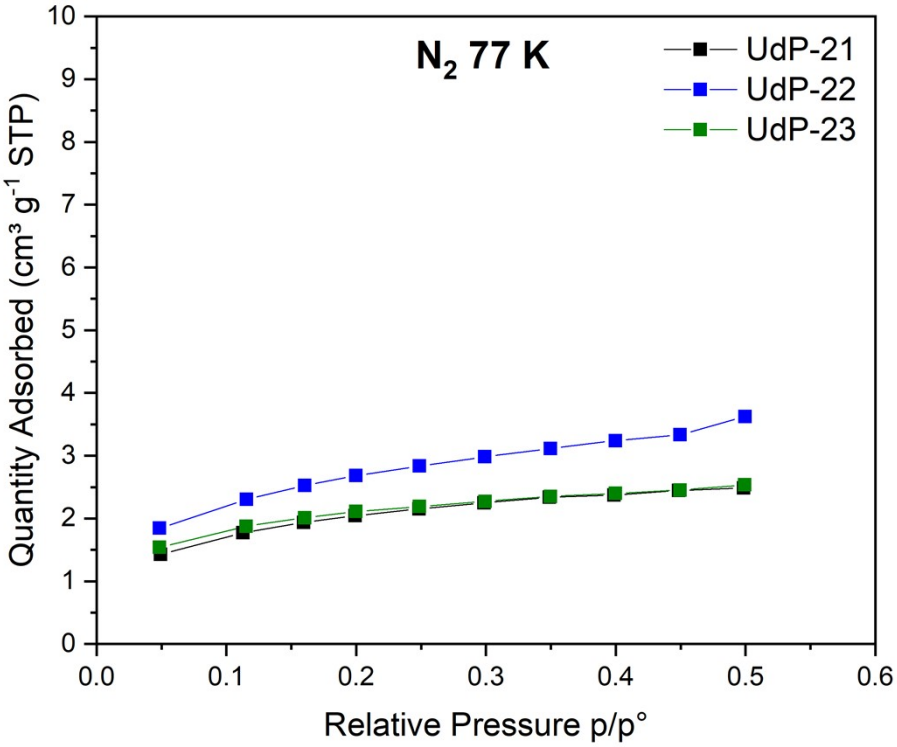

Figure S25. N_2 isotherms at 77 K of **UdP-21**, **UdP-22** and **UdP-23**

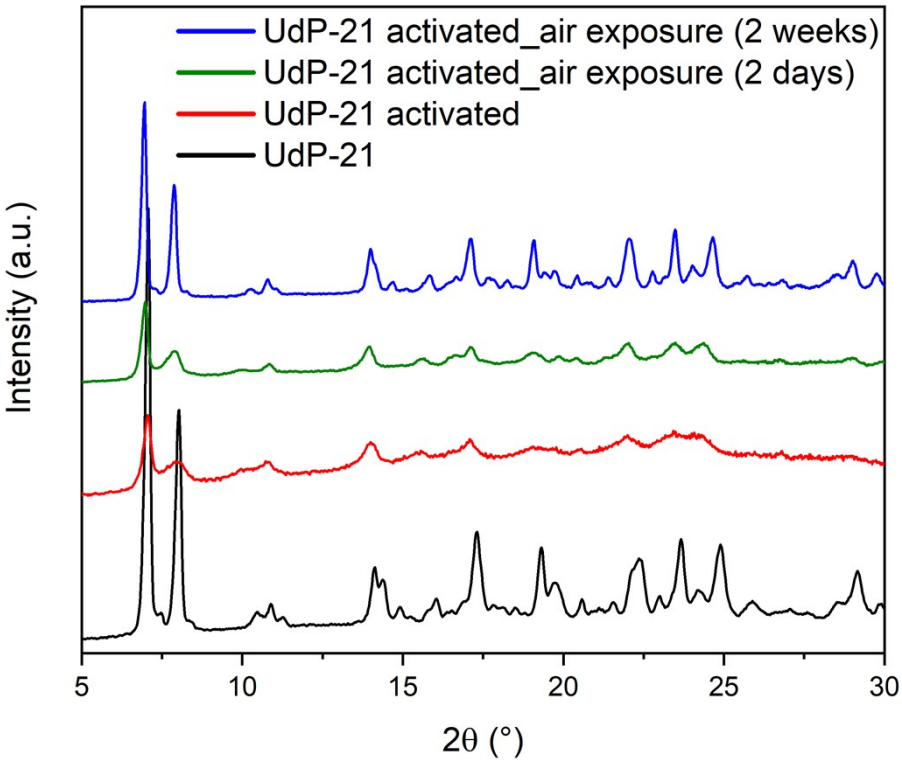

Figure S26. Comparison between PXRD patterns of **UdP-21**: as synthesised (black), after the activation process (353 K under vacuum for 8 hours, red), after the exposure of the activated material to moisture air (2 days, green; 2 weeks, blue).

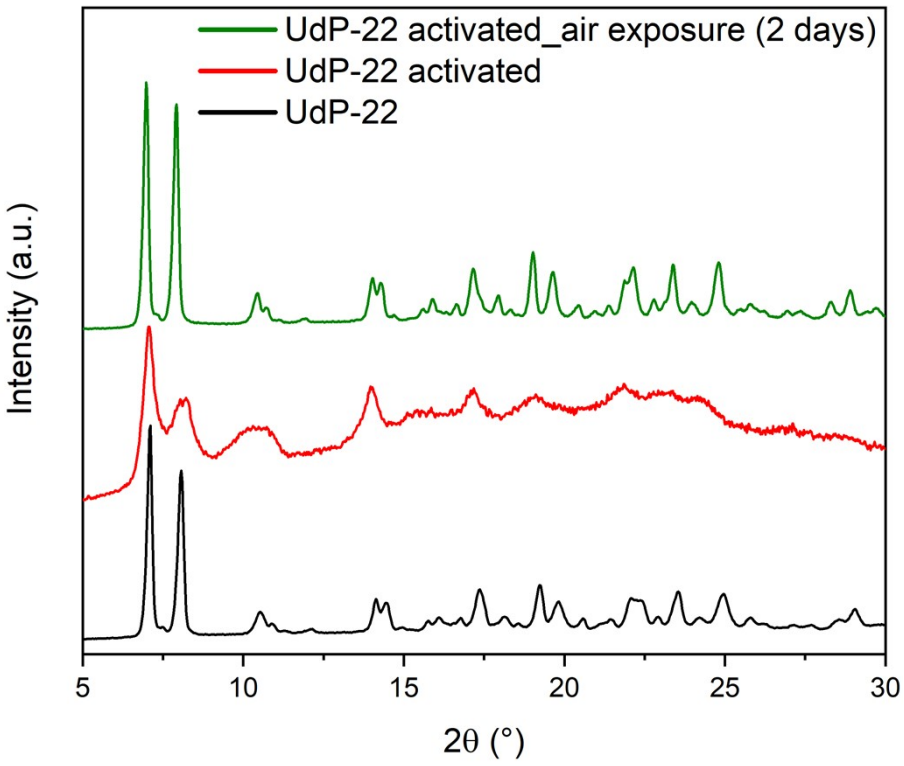

Figure S27. Comparison between PXRD patterns of **UdP-22**: as synthesised (black), after the activation process (353 K under vacuum for 8 hours, red), after the exposure of the activated material to moisture air for 2 days (green).

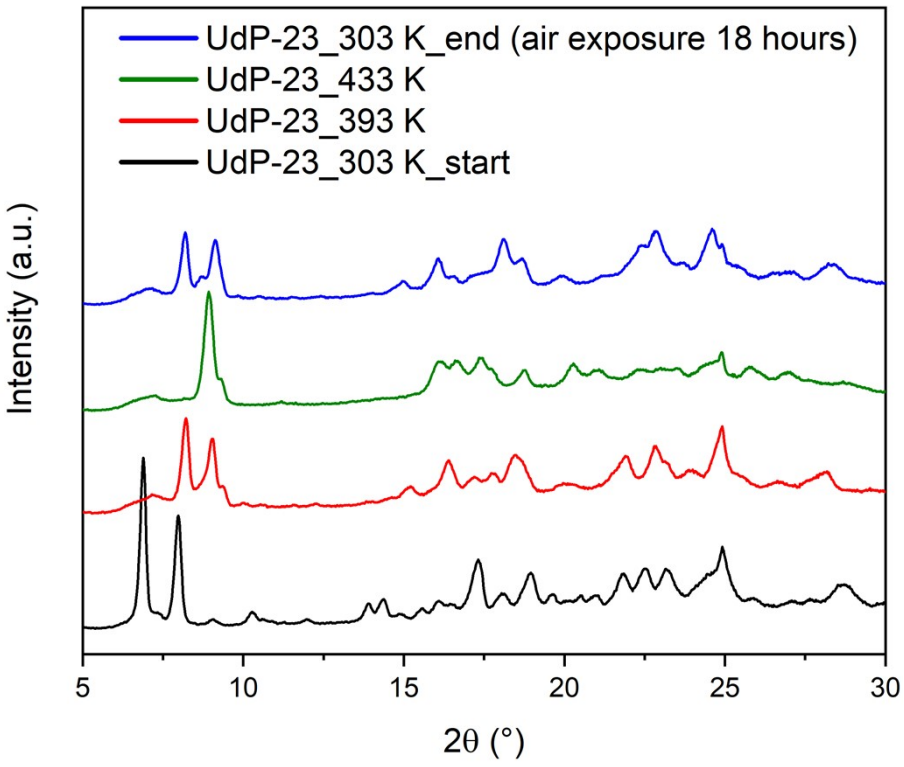

Figure S28. VT-PXRD patterns of **UdP-23** registered in air: as synthesised at 303 K (black), 393 K (red), 433K (green), 303 K 18 hours after the temperature ramp (blue).

Ligand characterisation

1,1'-(2-(trifluoromethyl)-1,4-phenylene)bis(1H-imidazole) (**bibCF$_3$**)

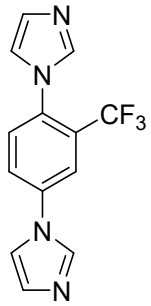

From 1,4-dibromo-2-(trifluoromethyl)benzene (5.00 g, 16.4 mmol). Reaction time 48 hours. Pale orange solid. Yield 3.30 g, 72%. ^{1}H NMR ($CDCl_3$): δ/ppm = 7.95 (br-s, 1 H, Im), 7.84 (d, 1 H, $^3J_{HH}$ = 2.6 Hz, C_6H_3), 7.71 (dd, 1 H, $^3J_{HH}$ = 2.6 Hz, $^4J_{HH}$ = 8.5 Hz, C_6H_3), 7.65 (br-s, 1 H, Im), 7.55 (d, 1 H, $^4J_{HH}$ = 8.5 Hz, C_6H_3), 7.36 (br-s, 1 H, Im), 7.29 (br-s, 1 H, Im), 7.23 (br-s, 1 H, Im), 7.14 (br-s, 1 H, Im); ^{13}C{^{1}H} NMR ($CDCl_3$): δ/ppm = 138.3 (Im), 138.0 (*ipso*-CN), 135.6 (Im), 134.2 (*ipso*-CN), 131.7 (Im), 131.5 (C_6H_3), 129.9 (Im), 128.9 (q, $^2J_{CF}$ = 30.4 Hz, *C*-CF_3), 125.2 (C_6H_3), 122.2 (q, $^1J_{CF}$ = 274.6 Hz, CF_3), 121.8 (Im), 120.1 (q, $^3J_{CF}$ = 5.8 Hz, C_6H_3), 118.0 (Im). ^{19}F{^{1}H} NMR ($CDCl_3$): δ/ppm = – 59.7 (s, 3 F, CF_3).

1,1'-(2-chloro-1,4-phenylene)bis(1H-imidazole) (**bibCl**)

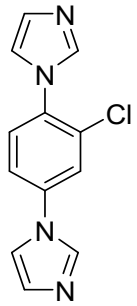

From 1,4-dibromo-2-chlorobenzene (4.33 g, 16.0 mmol). Reaction time 24 hours. White solid. Yield 2.85 g, 73%. ^{1}H NMR ($CDCl_3$): δ/ppm = 7.89 (br-s, 1 H, Im), 7.71 (br-s, 1 H, Im), 7.61 (d, 1 H, $^3J_{HH}$ = 2.4 Hz, C_6H_3), 7.47 (d, 1 H, $^4J_{HH}$ = 8.3 Hz, C_6H_3), 7.42 (dd, 1 H, $^3J_{HH}$ = 2.4 Hz, $^4J_{HH}$ = 8.4 Hz, C_6H_3), 7.30 (br-s, 1 H, Im), 7.24* (br-s, 1 H, Im), 7.16 (br-s, 1 H, Im). ^{13}C{^{1}H} NMR ($CDCl_3$): δ/ppm = 138.0 (C-Cl), 137.5 (Im), 135.5 (Im), 134.1 (*ipso*-CN), 131.5 (*ipso*-CN), 131.4 (Im), 129.9 (Im), 129.0 (C_6H_3), 123.5 (C_6H_3), 120.5 (C_6H_3 + Im), 118.0 (Im).*Partially hidden by solvent.

1,1'-(2-methyl-1,4-phenylene)bis(1H-imidazole) (**bibMe**)

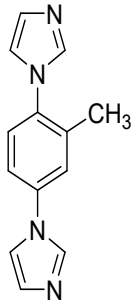

From 1,4-dibromo-2-methylbenzene (3.89 g, 15.6 mmol). Reaction time 48 hours. In this case, the reaction required 30 mol% of CuI. White solid. Yield 2.73 g, 78%. ^{1}H NMR ($CDCl_3$): δ/ppm = 7.88 (br-s, 1 H, Im), 7.60 (br-s, 1 H, Im), 7.38-7.33 (m, 3 H, C_6H_3), 7.30 (br-s, 1 H, Im), 7.23 (br-s, 2 H, Im), 7.07 (br-s, 1 H, Im), 2.26 (s, 3 H, Me); ^{13}C{^{1}H} NMR ($CDCl_3$): δ/ppm = 137.5 (Im), 136.3 (*ipso*-CN), 135.8 (*ipso*-CN), 135.6 (Im), 130.9 (*C*-Me), 129.9 (Im), 128.2 (C_6H_3), 124.0 (C_6H_3), 120.5 (Im), 119.8 (C_6H_3), 118. 2 (Im), 18.0 (CH_3).

1,1'-(2-methoxy-1,4-phenylene)bis(1H-imidazole) (**bibOMe**)

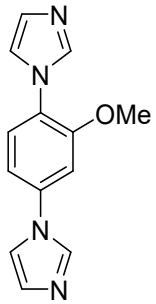

From 1,4-dibromo-2-methoxybenzene (4.25 g, 16.0 mmol). Reaction time 24 hours. Pale grey solid. Yield 2.60 g, 68%. ^{1}H NMR ($CDCl_3$): δ/ppm = 7.88 (br-s, 1 H, Im), 7.79 (br-s, 1 H, Im), 7.38 (d, 1 H, $^{4}J_{HH}$ = 8.4 Hz, C_6H_3), 7.31 (br-s, 1 H, Im), 7.24 (br-s, 1 H, Im), 7.21 (br-s, 1 H, Im), 7.19 (br-s, 1 H, Im), 7.07 (dd, 1 H, $^{3}J_{HH}$ = 2.4 Hz, $^{4}J_{HH}$ = 8.3 Hz, C_6H_3), 7.05 (d, 1 H, $^{3}J_{HH}$ = 2.2 Hz, C_6H_3), 3.91 (s, 3 H, OMe). ^{13}C{^{1}H} NMR ($CDCl_3$): δ/ppm = 153.7 (*ipso*-CO), 137.8 (Im), 135.7 (Im), 130.9 (Im), 129.3 (Im), 126.7 (C_6H_3), 125.8 (*ipso*-CN), 120.2 (Im + *ipso*-CN), 118.4 (Im), 113.9 (C_6H_3), 106.2 (C_6H_3), 56.3 (OMe).

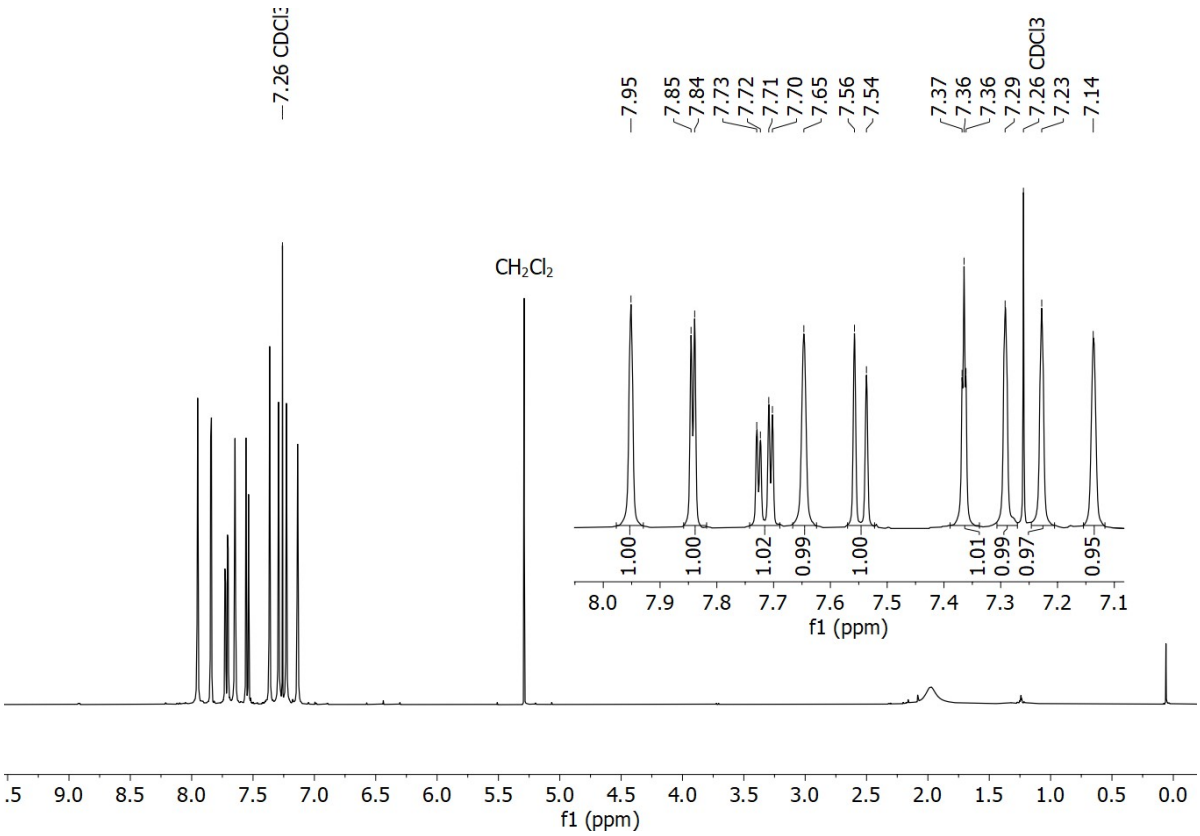

Figure S27. ^{1}H NMR spectrum (400 MHz, $CDCl_3$) of **bibCF$_3$**.

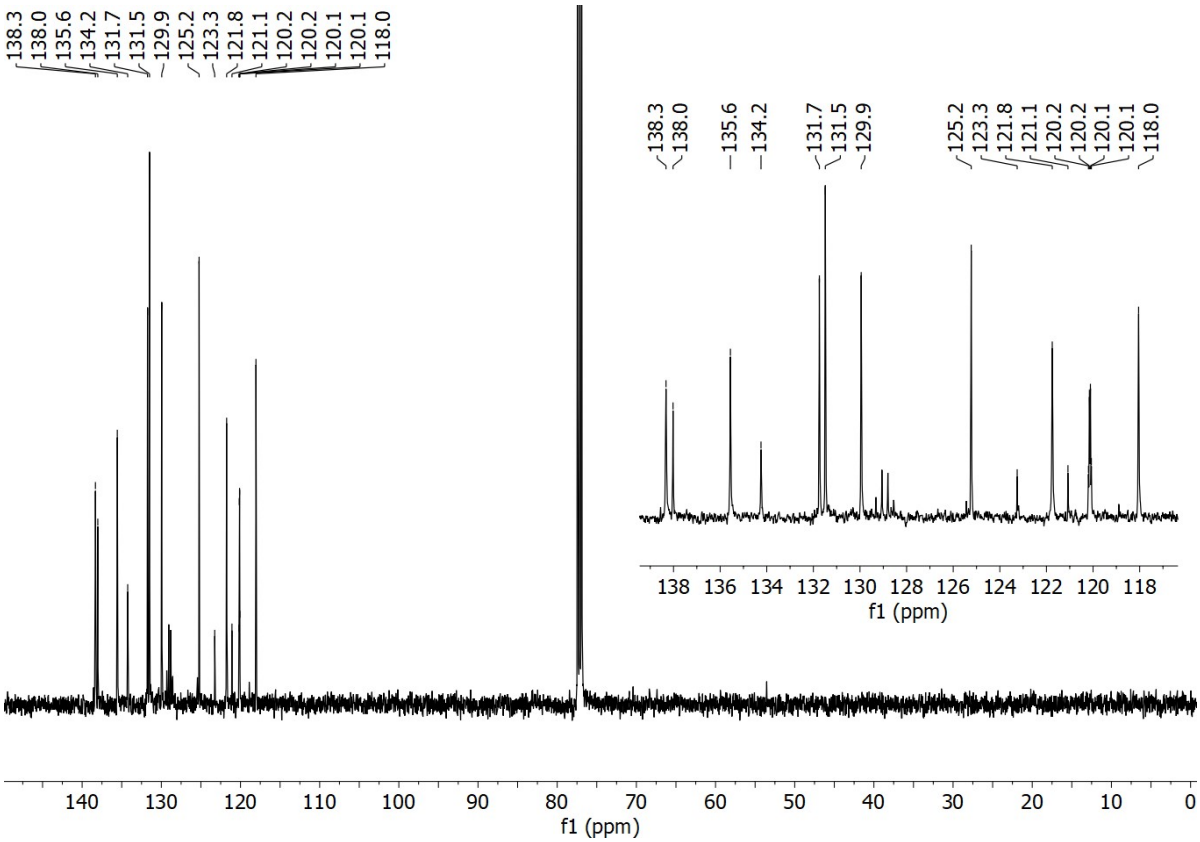

Figure S28. ^{13}C NMR spectrum (400 MHz, $CDCl_3$) of **bibCF$_3$**.

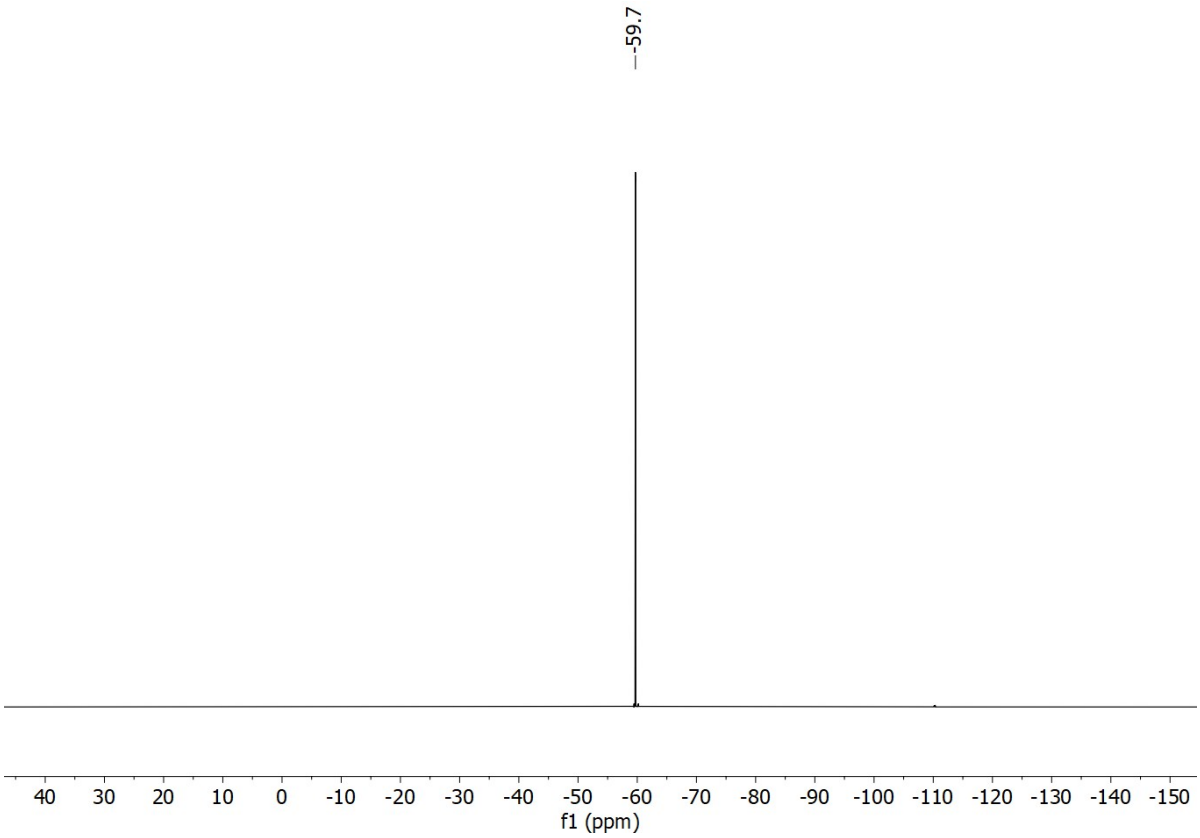

Figure S29. ^{19}F NMR spectrum (400 MHz, $CDCl_3$) of **bibCF$_3$**.

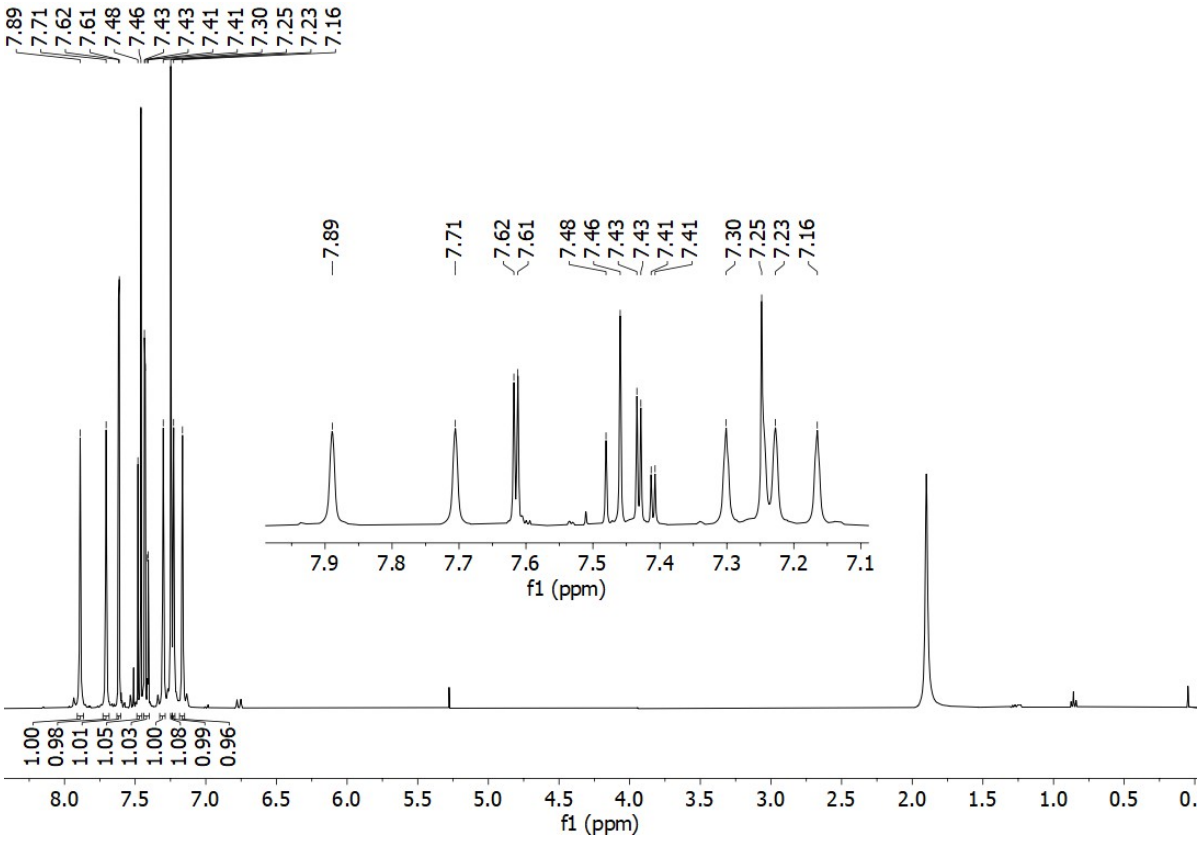

Figure S30. ^{1}H NMR spectrum (400 MHz, $CDCl_3$) of **bibCl**.

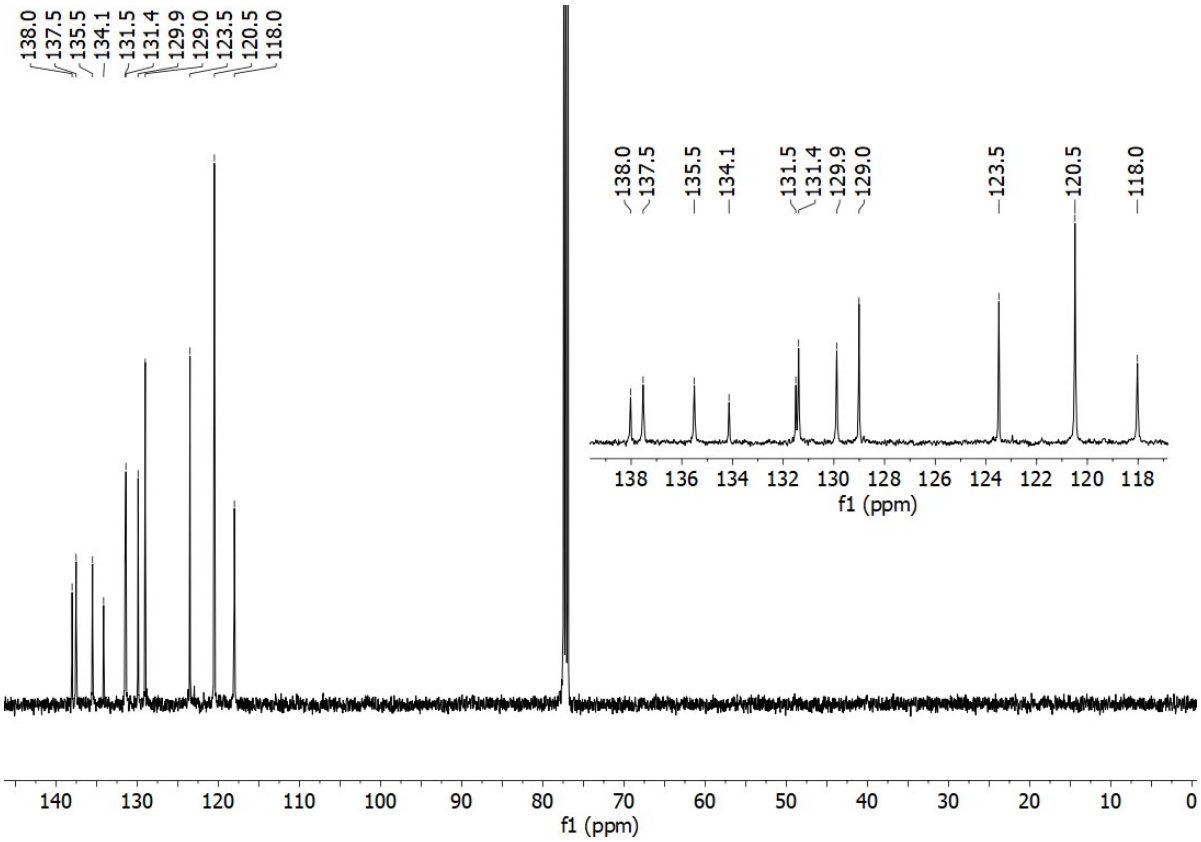

Figure S31. ^{13}C NMR spectrum (400 MHz, $CDCl_3$) of **bibCl**.

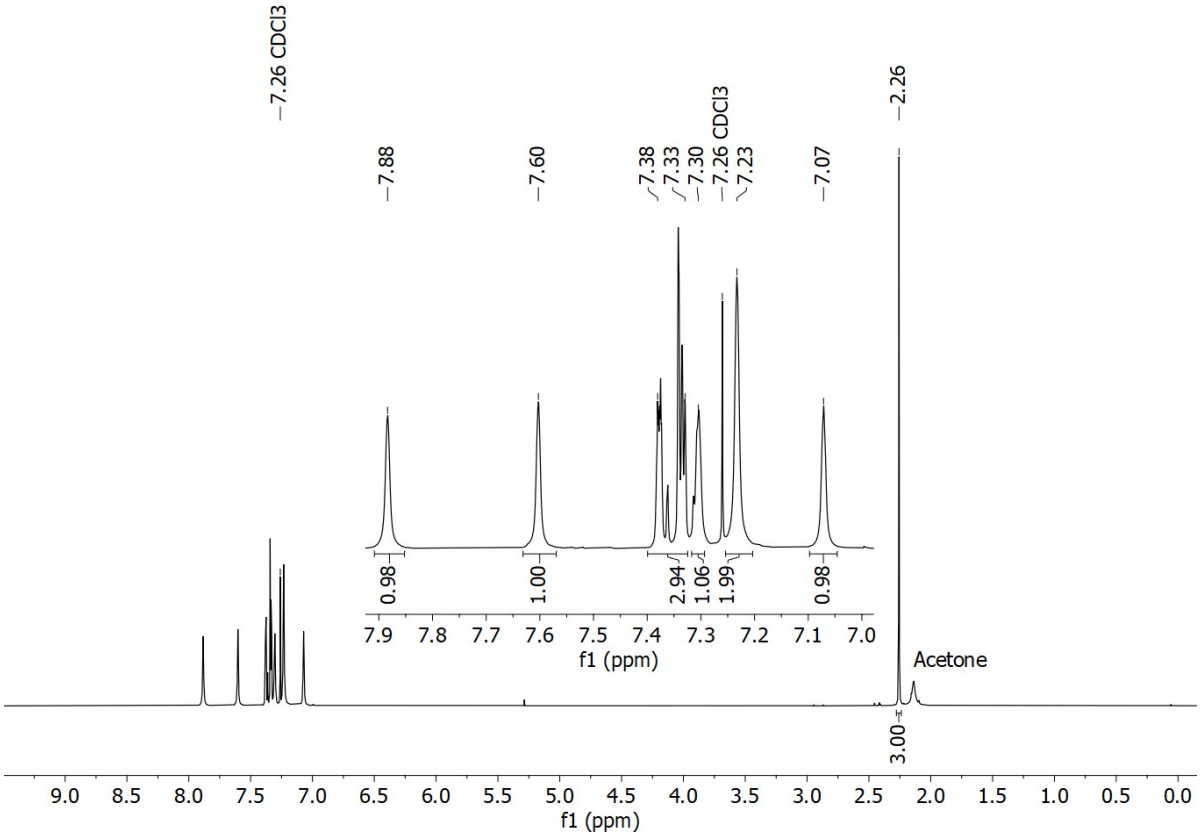

Figure S32. ^{1}H NMR spectrum (400 MHz, $CDCl_3$) of **bibMe**.

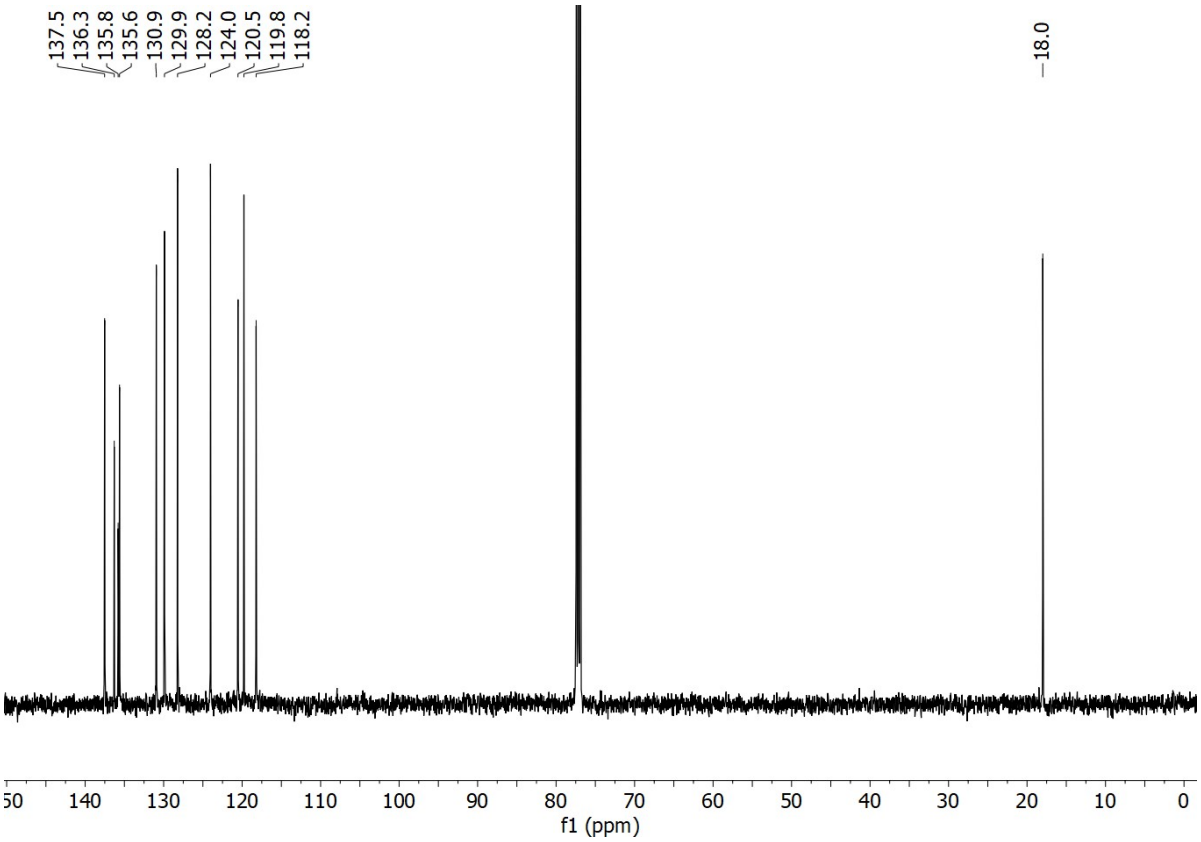

Figure S33. ^{13}C NMR spectrum (400 MHz, $CDCl_3$) of **bibMe**.

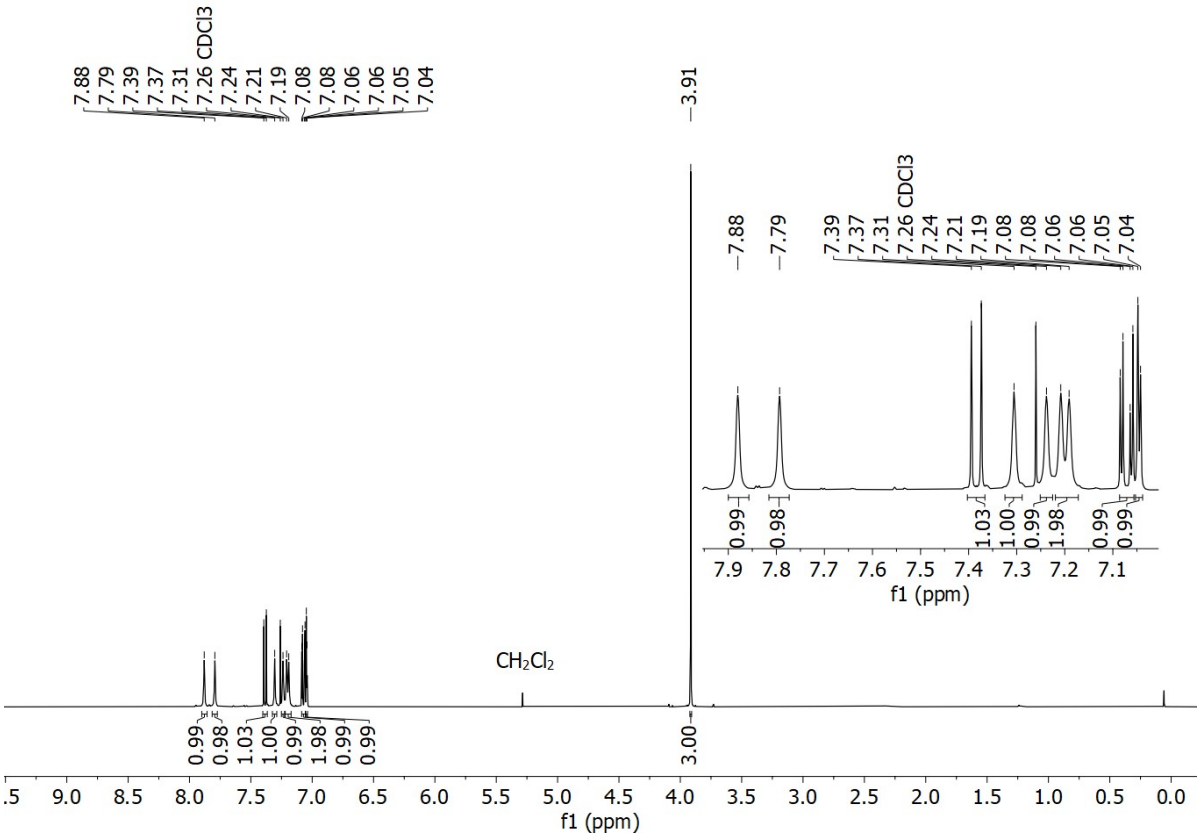

Figure S34. ^{1}H NMR spectrum (400 MHz, $CDCl_3$) of **bibOMe**.

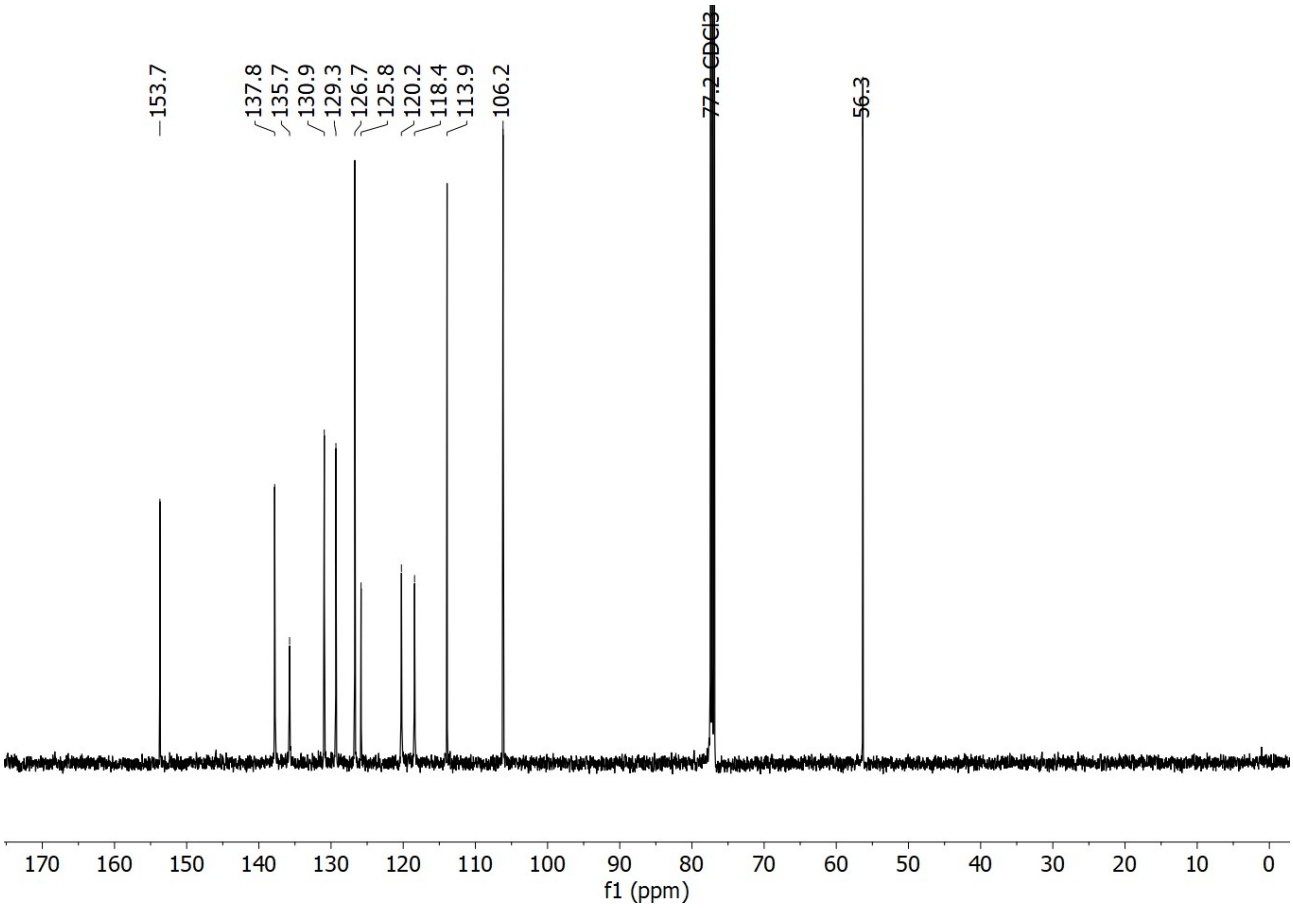

Figure S35. ^{13}C NMR spectrum (400 MHz, $CDCl_3$) of **bibOMe**.